Piezoelectrically Activated Resonant Bridge Microaccelerometer

David B. Hicks, Shih-Chia Chang, Michael W. Putty and David S. Eddy

Electrical and Electronics Department
General Motors Research and Development Center
Warren, MI 48090-9055

ABSTRACT

As the complexity of automotive systems increases, there has been a concurrent increase in demand for motion sensors. Vibratory sensors, capable of measuring linear and angular motion, have the potential of satisfying these demands. A resonant bridge microaccelerometer has been developed to test two design innovations. The first involves the incorporation of thin film zinc oxide to piezoelectrically excite and detect bridge resonance. The primary advantage of moving away from electrostatic excitation and detection to the piezoelectric approach is the elimination of squeeze-film damping. Higher Q values have been obtained as a result and offers the potential for device operation at reduced vacuum levels. The second innovation turns the device inside out by placing the proof mass around the perimeter of the device rather than at the center. This new cantilever-like configuration decouples the resonant bridges from the effects of package-induced stress and also provides a proof mass that is six times heavier than its central proof mass counterpart.

INTRODUCTION

Sensors based on beam resonance have attracted more and more attention over the past few years due to the quasi-digital nature of the output signal and the better sensitivity/bandwidth product of the sensors [1-4]. So far, beam resonance has been most often activated by electrostatic force. Simple device structure and IC process compatibility are the advantages of this approach. However, the close proximity of the beam to the drive-sense electrodes (~2 μm) necessitates vacuum packaging ($\leq$10 mTorr) to minimize squeeze film damping effects so as to achieve a high quality factor (Q). In addition, the electrically measured resonant frequency is a strong function of the electrode gap distance, and hence, it is more sensitive to processing variations associated with the construction of resonant structures [5].

As an alternative to electrostatics, we have experimented with sputter-deposited zinc oxide (ZnO) thin films to piezoelectrically drive and sense bridge resonance. With drive voltages of a few millivolts, a clear bridge resonance was observed even at one atmosphere. The measured Q value was 300. Q increased to 1800 when the measurement was done under a vacuum of ~100 mTorr, which is two to three times greater than the Q values achieved with the electrostatically driven devices. In this work, the established ZnO thin film technology is applied to the fabrication of a resonant bridge microaccelerometer. Simple on-chip circuitry, consisting of a diode and a n-channel depletion mode MOSFET is incorporated for signal conditioning and amplification.

SENSOR CONCEPT

The device is a two-axis accelerometer which employs two pairs of silicon bridges orthogonally attached to a common proof mass to measure in-plane acceleration. This acceleration causes differential axial loads on opposing bridge pairs, thereby shifting their resonant frequencies. The acceleration component aligned with a pair is measured by the difference in resonant frequencies. By monitoring both bridge pairs simultaneously, direction can also be determined. In-depth discussions on the device concept and theory of operation have been reported previously [4].

In this version of the accelerometer, bridge resonance is driven and detected piezoelectrically. When an electric field is applied vertically across the ZnO drive element, a stress is induced in the film laterally (through piezoelectric coupling, d_{31}). This stress bends the bridge which, in turn, produces a strain in the sensing element. The resulting change in the charged state of the ZnO sensing element is detected and amplified by the on-chip circuitry.

DEVICE DESCRIPTION

Plan and cross-sectional views of the overall structure of the accelerometer are shown in Fig. 1 (a-c). The dimensions of the various components are given below, along with brief descriptions:

1. Proof mass

12 mg (peripheral)   2 mg (central)

Two different proof mass arrangements were devised: a central proof mass (Fig. 1b), and a peripheral proof mass (Fig. 1c). For a given chip size, the peripheral proof mass is approximately six times heavier than the central proof mass which translates into greater sensitivity. The accelerometer with the peripheral proof mass is essentially a released structure and inherently is less affected by package-induced stress.

2. Drive-Sense Elements

thickness = 1 μm   area = 9600 μm^2 (per pad)

The transducing elements are positioned in two different configurations as shown in Figs. 2a and 2b. In both cases, the ZnO pads are positioned such that they do not cross the points of inflection of the fundamental flexure mode of the bridge. The configuration shown in Fig. 2b provides a larger ZnO area, and, hence, a larger sensor signal is expected. The drive and sense elements are sandwiched between silicon dioxide and silicon nitride layers to prevent charge leakage, thus ensuring device performance in the low frequency spectrum.

3. Bridges

	Length	Width	Thickness
Resonant bridge:	500 μm	100 μm	5 μm
Constraining bridge:	1200 μm	100 μm,	10 μm

The resonant bridges as well as the constraining bridges are made of heavily boron-doped single crystal silicon.

0-9640024-0-X/hh1994/$20©1994TRF
DOI 10.31438/trf.hh1994.51

FABRICATION

Figure 3 shows the principal processing steps in sequence. The thicknesses of the resonant and constraining bridges are defined by two separate deep boron diffusion operations (Fig. 3a). The on-chip circuitry (a diode and a n-channel depletion mode MOSFET) is closely positioned to the resonant bridge with the diode-gate lead connected to the sensing element (Fig. 3b). The ZnO pads are deposited by rf magnetron sputtering and patterned with either phosphoric acid or ammonium chloride etchants [6]. The ZnO is sandwiched between a silicon dioxide layer and a plasma nitride layer before aluminum metallization (Fig. 3c). The proof mass, resonant and constraining bridges are formed simultaneously by etching in an ethylene diamine-pyrocatechol (EDP) etchant (Fig. 3d). Figures 4a and 4b are photomicrographs of the fabricated accelerometers showing both proof mass configurations.

RESULTS AND DISCUSSION

Figures 5a and 5b show the frequency response of the resonant bridge associated with the central proof mass when operated at one atmosphere and at 100 mTorr, respectively. Bridge resonance is clearly detected at one atmosphere, however, the quality factor (Q) is low. Q increases to 1,800 when the device is operated at 100 mTorr. Similar results are obtained for the device with a peripheral proof mass. The measured resonant frequency, f_m, is $\geq$200 kHz, which is somewhat higher than the expected natural frequency, f_o, of an unstressed bridge as estimated by the equation,

$$f_o = 1.03\sqrt{\frac{E}{(1-\nu^2)\rho}}\left(\frac{t}{l^2}\right) \qquad (1)$$

where E is Young's modulus, ν is Poisson's ratio, ρ is the density, t is the bridge thickness, and l is the length of the bridge. Neglecting the effects of the various layers comprising the bridge and using $E = 1.5x10^{12}\ dyne/cm^2$, $\nu = 0.25$, $\rho = 2.328\ g/cm^3$, $t = 5\mu m$, and $l = 500\mu m$, the calculated resonant frequency is ~165 kHz. The built-in tensile stress can be estimated from the following relationship,

$$f_m = f_o\sqrt{1+0.293\left(\frac{\sigma}{E}\right)\left(\frac{l}{t}\right)^2} \qquad (2)$$

and comes out to be $\sim 2x10^6\ dyne/cm^2$, which is comparable to the values reported by Ding, et al, for heavily boron-doped silicon [7].

Figures 6a and 6b show single-bridge responses to static in-plane accelerations of $\pm$1g for the different proof mass configurations. The measured frequency shifts are ~36 Hz and 12 Hz for devices with the peripheral proof mass and central proof mass, respectively, as compared with the calculated values of 130 Hz and 20 Hz. The causes of these large discrepancies between the measured and calculated responses are not clear at this point. It may be attributed to the fact that the resonant bridge is formed by five layers of different materials: B^+ doped silicon / silicon dioxide / ZnO / plasma nitride / aluminum.

CONCLUDING REMARKS

The results obtained in this work clearly demonstrate that piezoelectric thin film ZnO is a viable transduction material for a resonant bridge accelerometer and that sensor designs exploiting the piezoelectric effect offer some advantages over prior developments using electrostatics. In the piezoelectric design, the electrodes are an integral part of the resonant bridge, thus eliminating the bridge-to-electrode air gap required for electrostatic devices. Consequently, device performance is not limited by squeeze film damping nor by nonlinear effects associated with changing air gap dimensions. When measuring the quality factor (Q) for both devices at 100 mTorr, the new device yields 5 times the Q value of its electrostatic predecessor. The direct benefit of the new design is that vacuum packaging requirements may be relaxed -- or eliminated -- for some applications.

Finally, there are two advantages to the peripheral proof mass configuration: a) it eliminates the coupling of package-induced stress to the resonant bridges which simplifies the packaging process, and b) it yields a heavier proof mass for a given die size when compared to its central proof mass counterpart, thus making more efficient use of silicon real estate.

REFERENCES

1. W. Yun and R. T. Howe, "Recent Development in Silicon Microaccelerometers," *Sensors, 9, 10* (1992) p. 31.

2. S. Bouwstra, R. Legtenberg, H. A. C. Tilmans and M. Elwenspeck, "Resonating Microbridge Mass Flow Sensor," *Sensors and Actuators, A21-A23* (1991) p. 332.

3. R. A. Buser and N. F. Derooij, "Very High Q-factor Resonators in Monocrystalline Silicon," *Sensors and Actuators, A21-A23* (1991) p. 323.

4. S. C. Chang, M. W. Putty, D. B. Hicks, C. H. Li and R. T. Howe, "Resonant-Bridge Two-axis Microaccelerometer." *Sensors and Actuators, A21-A23* (1991) p. 342.

5. M. W. Putty, D. B. Hicks, S. C. Chang, "An Integrated Microaccelerometer for Automotive Sensing Applications," *GM Internal Research Report* (1990).

6. S. C. Chang, D. B. Hicks and R. C. O. Laugal, "Patterning of Zinc Oxide Thin Films," *Technical Digest, IEEE Solid-State Sensor and Actuator Workshop, Hilton Head, SC, 1992,* p. 41.

7. X. Ding, W. H. Ko, Y. Niu and W. He. "A Study on Silicon-Diaphragm Buckling," *Technical Digest, IEEE Solid-State Sensor and Actuator Workshop, Hilton Head, SC, 1990,* p. 128.

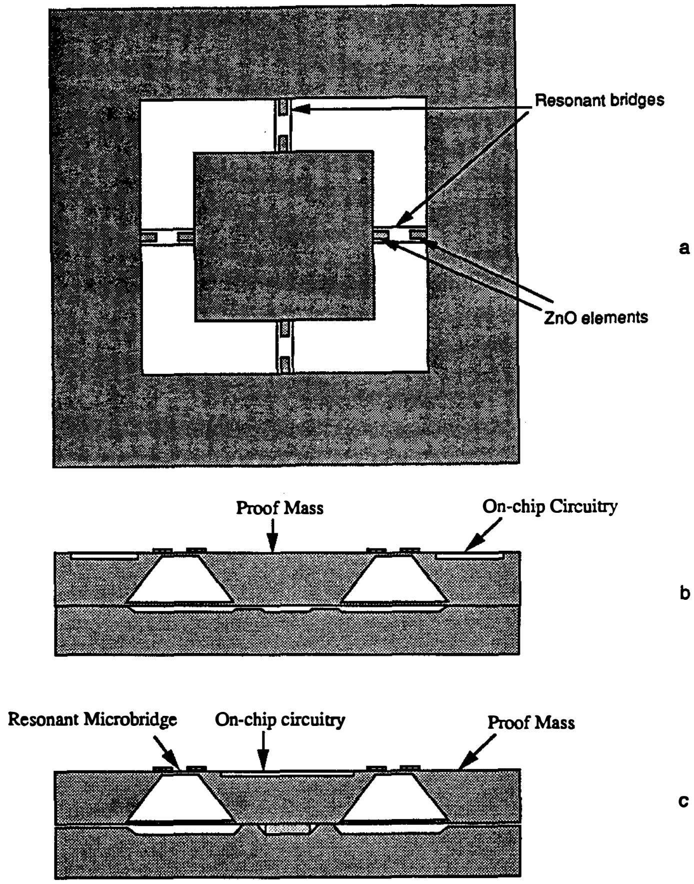

Fig. 1 Schematic diagram of a piezoelectrically driven and sensed resonant bridge microaccelerometer with alternative proof mass configurations: a) top view, b) cross sectional view of central proof mass configuration, c) cross sectional view of peripheral proof mass configuration.

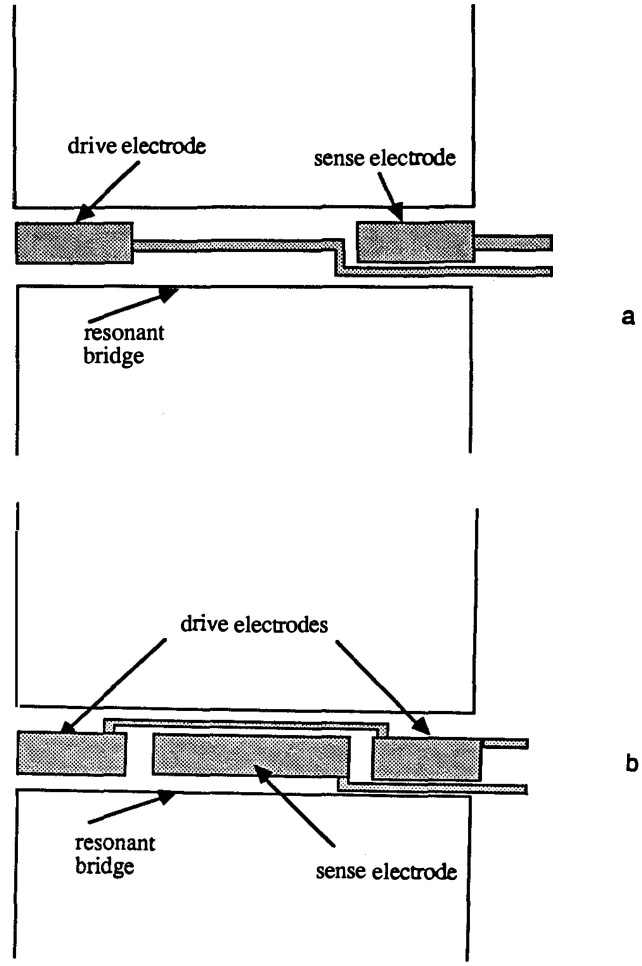

Fig. 2 Two different arrangements of thin film zinc oxide transducing elements.

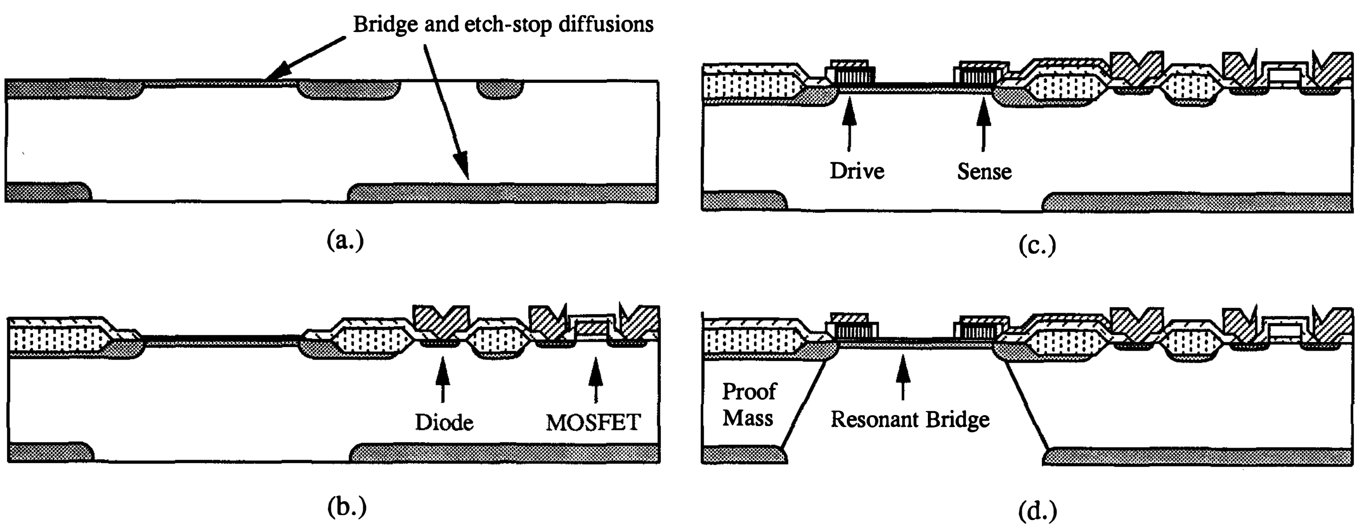

Fig. 3 Major processing steps for device fabrication: a) the dimensions of the resonant and constraining bridges are defined by two consecutive boron diffusions, b) the on-chip circuitry consists of a diode and a depletion mode n-channel MOSFET, c) the ZnO thin films are sandwiched between SiO_2 and Si_3N_4 to prevent charge leakage, d) proof mass, constraining bridges and resonant bridges are formed simultaneously by etching in EDP.

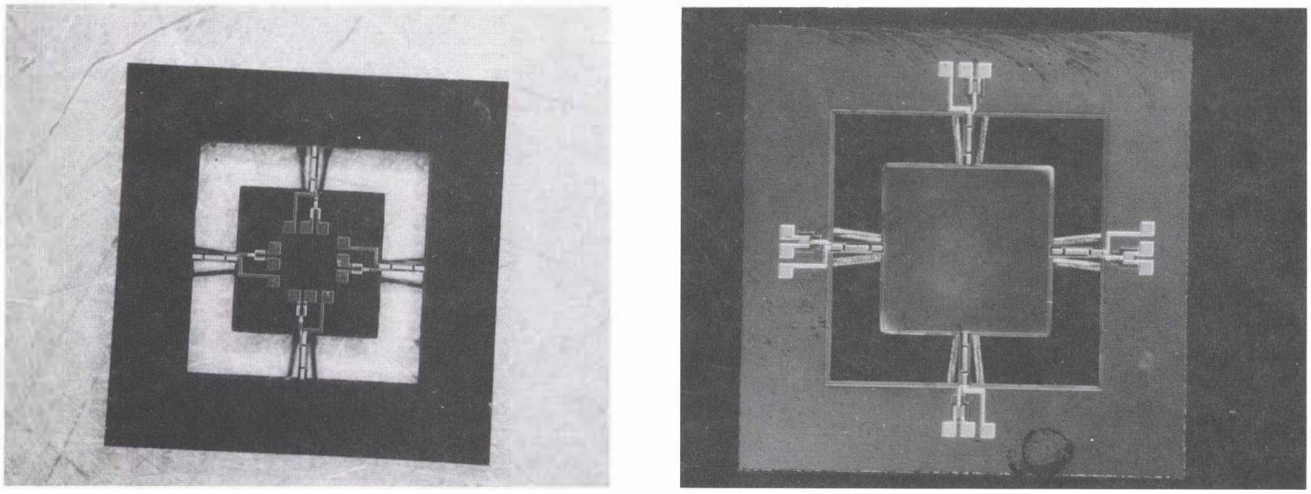

Fig. 4 Photographs of fabricated microaccelerometers: a) peripheral proof mass configuration, b) central proof mass configuration.

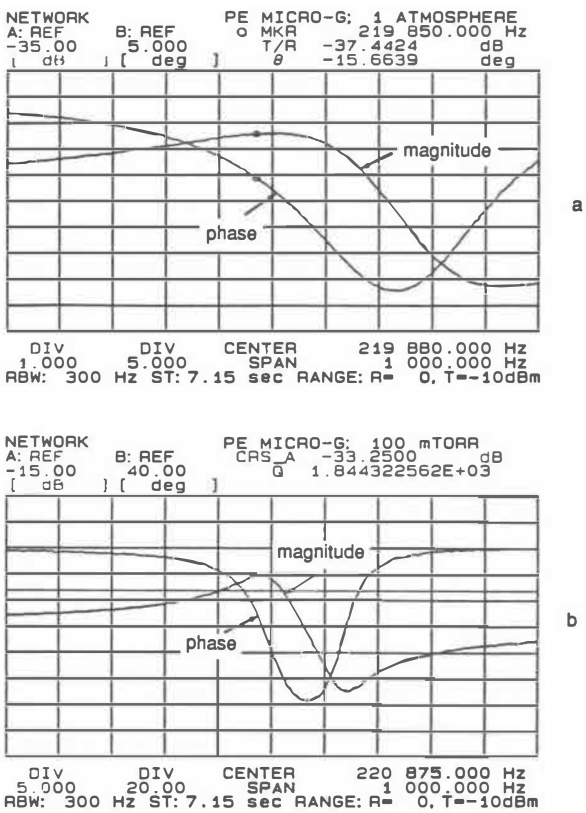

Fig. 5 Frequency responses of the resonant bridge associated with central proof mass when operated at: a) one atmosphere pressure, and b) 100 mTorr.

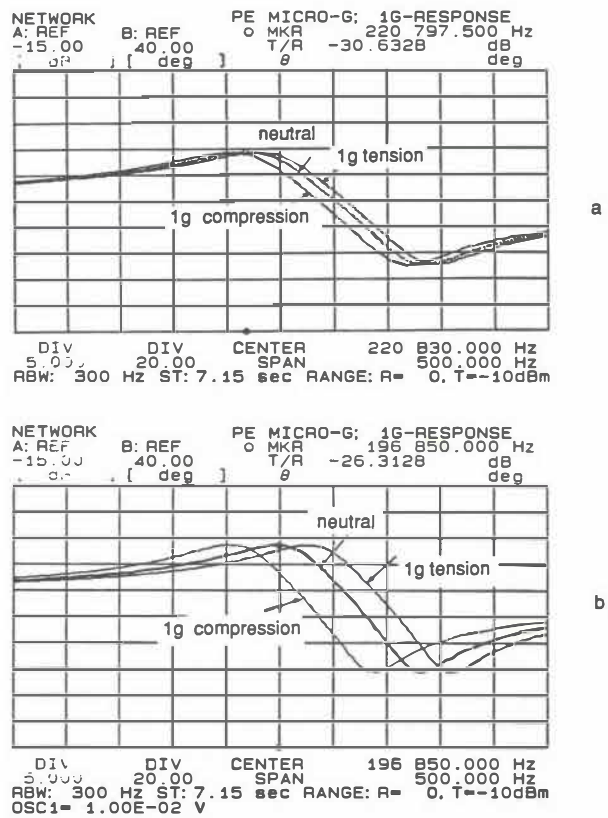

Fig. 6 Frequency shifts of the resonant bridges when the proof mass is subjected to static acceleration of ± 1g in the direction parallel to the length of the bridge: a) central proof mass configuration, Δf = 12 Hz, b) peripheral proof mass configuration, $\Delta f = 36$ Hz.